International Journal of Pharmaceutics 387 (2010) 236–243

Contents lists available at ScienceDirect

International Journal of Pharmaceutics

journal homepage: www.elsevier.com/locate/ijpharm

Pharmaceutical Nanotechnology

Ascorbyl dipalmitate/PEG-lipid nanoparticles as a novel carrier for hydrophobic drugs

Kunikazu Moribe[a,*], Sunao Maruyama[a], Yutaka Inoue[b], Toyofumi Suzuki[c], Toshiro Fukami[c], Kazuo Tomono[c], Kenjirou Higashi[a], Yuichi Tozuka[d], Keiji Yamamoto[a]

[a] Graduate School of Pharmaceutical Sciences, Chiba University, 1-33 Yayoi-cho, Inage-ku, Chiba 263-8522, Japan
[b] Faculty of Pharmaceutical Sciences, Josai University, 1-1 Keyakidai, Sakado-shi, Saitama 350-0295, Japan
[c] College of Pharmacy, Nihon University, 7-7-1 Narashinodai, Funabashi, Chiba 274-8555, Japan
[d] Gifu Pharmaceutical University, 5-6-1, Mitahora-higashi, Gifu 502-8585, Japan

ARTICLE INFO

Article history:
Received 24 August 2009
Received in revised form
20 November 2009
Accepted 4 December 2009
Available online 18 December 2009

Keywords:
Ascorbyl dipalmitate
DSPE–PEG
Nanoparticle
Complex
Amphotericin B

ABSTRACT

L-Ascorbyl 2,6-dipalmitate (ASC-DP), a fatty ester derivative of ascorbic acid, is poorly soluble in water and does not spontaneously form micelles or liposomal structures in water. In this study, we attempted to prepare an ASC-DP/surfactant nano-sized complex as a carrier for hydrophobic drugs. Samples were prepared by hydrating a solvent-evaporated film of ASC-DP/surfactant at a molar ratio of 1:1. Among the surfactants tested, distearoylphosphatidylethanolamine-polyethylene glycol 2000 (DSPE-PEG) was found to form stable nanoparticles with ASC-DP (average particle size: ca. 67 nm). Several hydrophobic drugs were incorporated in the ASC-DP/DSPE-PEG nanoparticles. Stability, toxicity, and blood residence of the drug-containing ASC-DP/DSPE-PEG nanoparticles were evaluated using amphotericin B (AmB) as the model drug. By intravenously administering mice with the formulations, we determined the minimum lethal dose of Fungizone®, a formulation of AmB solubilized with sodium deoxycholate, was 3.0 mg/kg, while that of AmB/ASC-DP/DSPE-PEG nanoparticles was 10.0 mg/kg. When 2.0 mg/kg, Fungizone® was administered, the mice showed higher renal and hepatic toxicities. Intravenously administered AmB/ASC-DP/DSPE-PEG nanoparticles demonstrated higher concentration in plasma than Fungizone®. Thus, the ASC-DP/DSPE-PEG nanoparticle system appears to be a promising delivery system for hydrophobic drugs.

1. Introduction

Many nanoparticle carriers have been developed as drug-delivery systems (DDSs). Liposomes (Yamada and Harashima, 2008), micelles (Sawant et al., 2006; Nishiyama and Kataoka, 2006), and nanospheres (Yamamoto et al., 2005) have been widely investigated to examine if they selectively accumulate at the target site, which is a requirement for effective therapeutic efficacy with reduced toxicity. Encapsulation of an active pharmaceutical ingredient (API) can be a hurdle when formulating nanoparticles. For example, liposome formulations can encapsulate both hydrophilic and hydrophobic drugs. However, both the encapsulated amount and stability of the formulation tend to depend on the physicochemical properties of the API. In the case of polymeric micelles or nanospheres, selecting appropriate excipients is important for miscibility or specific interaction with the API.

An antioxidant is usually loaded to a nanoparticle formulation to prevent oxidation of the API as well as of carrier components (Fočo et al., 2005; Ratnam et al., 2006). Ascorbic acid is a widely used hydrophilic antioxidant. However, since ascorbic acid is unstable in water, many ascorbic-acid derivatives have been synthesized (LoNostro et al., 2000; Takebayashi et al., 2006; Teeranachaideekul et al., 2008). The practical uses of ascorbic-acid derivatives not only as antioxidants but also as food or pharmaceutical excipients have been examined (Fočo et al., 2005; Llabot et al., 2007). Ascorbic acid 2-glucoside (AA-2G) is a newly approved food additive. It has high stability against thermal and oxidative degradation and is rapidly converted to ascorbic acid by α-glucosidase in the blood and liver (Yamamoto et al., 1990; Matsukawa et al., 2000). Inoue et al. reported that it can also be used to solubilize APIs (Inoue et al., 2007). A variety of alkyl chains that form the ester linkage with ascorbic acid can be used to improve surface activity. Ascorbyl monoalkylated derivatives, such as octanoyl-6-*O*-ascorbic acid and ascorbyl palmitate, can be used to develop micelles (Bilia et al., 2002), microemulsions (Špiclin et al., 2001), and liposomal formulations (Gopinath et al., 2004).

* Corresponding author. Tel.: +81 43 290 2938; fax: +81 43 290 2939.
E-mail address: moribe@p.chiba-u.ac.jp (K. Moribe).

0378-5173/$ – see front matter © 2009 Elsevier B.V. All rights reserved.
doi:10.1016/j.ijpharm.2009.12.007

L-Ascorbyl 2,6-dipalmitate (ASC-DP) is a fatty ester derivative of ascorbic acid, with extremely low water solubility. The antioxidant has been used in cosmetics (Lien et al., 1993; Tanaka and Yamamoto, 1996). As compared with ascorbyl palmitate, ASC-DP cannot form micelles or liposomal structures on its own. However, the ASC-DP/distearoylphosphatidylethanolamine-polyethylene glycol 2000 (DSPE-PEG) complex forms stable nanoparticles. In this study, we prepared drug-containing ASC-DP/DSPE-PEG nanoparticles and investigated their physical stability. We attempted to incorporate several drugs into the nanoparticles. Amphotericin B (AmB), a polyene macrolide antibiotic drug used for systemic invasive fungal infection, was selected as the model drug because it specifically interacts with DSPE-PEG (Moribe et al., 1998). The intermolecular interaction is believed to contribute to effective AmB incorporation into the ASC-DP/DSPE-PEG nanoparticles. We also investigated the stability, toxicity, and blood residence of the AmB/ASC-DP/DSPE-PEG nanoparticles.

2. Materials and methods

2.1. Materials

ASC-DP, L-ascorbyl-6-dipalmitate (ASC-P), L-ascorbyl-2,6-dibutylate (ASC-DB), vitamin D_3, and 4-nitro-1-naphthylamine were obtained from Tokyo Chemical Industry, Co. Ltd., Japan. Distearoylphosphatidylcholine (DSPC), distearoyl glycerol PEG 2000 (DSG-PEG), and DSPE-PEG were purchased from NOF corporation (Japan). Sodium dodecyl sulfate (SDS), cetyltrimethyl ammonium bromide (CTAB), polyoxyethylene stearyl ether (Brij®78), acetohexamide, fluconazole, coenzyme Q_{10}, and AmB were obtained from Wako Pure Chemicals (Japan). Nystatin and thioctic acid were purchased from Sigma–Aldrich, Japan and Nacalai Tesque Inc., Japan, respectively. Fungizone® and clarithromycin were supplied by Bristol-Myers Squibb Company (USA) and Taisho Pharmaceutical Co. Ltd. (Japan), respectively. Other chemicals were of reagent grade and used without further purification.

2.2. Preparation of ASC-DP/DSPE-PEG or drug/ASC-DP/DSPE-PEG nanoparticles

ASC-DP and DSPE-PEG dissolved in chloroform were mixed in the molar ratio of 1:1. To prepare drug-incorporated samples, 10 mol% of the drug dissolved in an organic solvent was added to the chloroform solution. The solvent was evaporated with a rotary evaporator and further removed by drying in a desiccator under reduced pressure for 12 h. The film that formed on the pear-shaped flask was hydrated with distilled water to prepare nanosuspensions.

2.3. Retention of calcein in liposome

Retention of calcein in ASC-DP-incorporated liposomes was investigated to evaluate the miscibility of ASC-DP with the phospholipid bilayer. DSPC dissolved in chloroform was added in a flask, and the organic solvent was evaporated using a rotary evaporator. The film that formed was hydrated with 1.0 mL of phosphate-buffered saline (PBS, pH 7.4) containing 50-mM calcein. Hydrated samples were passed through a 200-nm polycarbonate membrane filter 5 times. Non-encapsulated calcein was removed by column separation. The fluorescence intensities of the calcein (excitation wavelength: 490 nm, emission wavelength: 520 nm) encapsulated in the ASC-DP-incorporated liposomes was measured at 25 °C under the same lipid concentration before and after disruption of the liposomes with 1.0% Triton X-100. Calcein retention was calculated using the following equation:

$$\text{retention of calcein}\,(\%) = \frac{I_a - I_b}{I_{0a} - I_{0b}} \times 100$$

where I_b and I_a are fluorescence intensities before and after disruption of the ASC-DP-incorporated liposomes. I_{0a} and I_{0b} are the fluorescence intensities of DSPC liposomes without ASC-DP.

2.4. Particle size analysis

The mean particle size of the nanoparticles was determined with the dynamic light-scattering method, using Microtrac UPA® (Nikkiso, Japan; measurement range: 0.003–6 μm).

2.5. Stability study

Stability studies of sample solutions were conducted during the particle size analysis after the storage at 25 °C for a definite time period.

2.6. Zeta potential measurement

A zeta potential for each suspension was determined using NICOMP 380ZLS® (Agilent Technologies Inc., USA). The measurements were repeated 3 times, and average values were calculated.

2.7. Experimental animals

For the in vivo toxicity experiment, male ddY mice (11–12 weeks old) were obtained from Japan SLC, Inc. (Japan). Male ddY mice (7 weeks old) were used for blood concentration measurement. The experiments were conducted according to guidelines approved by the Nihon University Animal Care and Use Committee (Nihon University, Japan). The mice were fed and given water ad libitum prior to the experiments.

2.8. Acute toxicity

The AmB/DSPE-PEG micelle solution and AmB/ASC-DP/DSPE-PEG nanoparticle suspension were prepared according to the hydration method mentioned above, except that sample films were hydrated with 9% sucrose solution to keep the isotonic condition and prevent AmB precipitation (Moribe et al., 1998). The mice were intravenously administered sample solutions including Fungizone® in increasing doses of AmB (0.5, 1, 2, 3, 4, 8, 10, and 12 mg/kg). To determine the minimum lethal dose (MLD), which was defined as the minimum dose that produces death in all mice, survival was checked for 3 h after injection.

2.9. Assessment of in vivo renal and hepatic toxicity

Sample solutions were prepared as described in Section 2.8 and intravenously injected into mice via the tail vain at a dose of 1.0 or 2.0 mg AmB/kg body weight. At 48 h after injection, blood samples were collected by cardiac puncture from anesthetized mice, and serum samples were separated by centrifugation. Serum creatinine (sCr) and blood urea nitrogen (BUN) levels of the mice treated with the samples were monitored to evaluate renal toxicity. The sCr and BUN levels were measured by the Jaffe method with a Wako creatinine test and by the urease indophenol method with a Wako nitrogen B test (Wako Pure Chemicals, Japan), respectively. Aspartate aminotransferase (AST) and alanine aminotransferase (ALT) were measured by a transaminase CII-test Wako (Wako Pure Chemicals, Japan) to evaluate hepatic toxicity. sCr, BUN, and AST and ALT were quantified spectrophotometrically at 520, 570, and 555 nm, respectively. Data was analyzed using the Student's *t*-test.

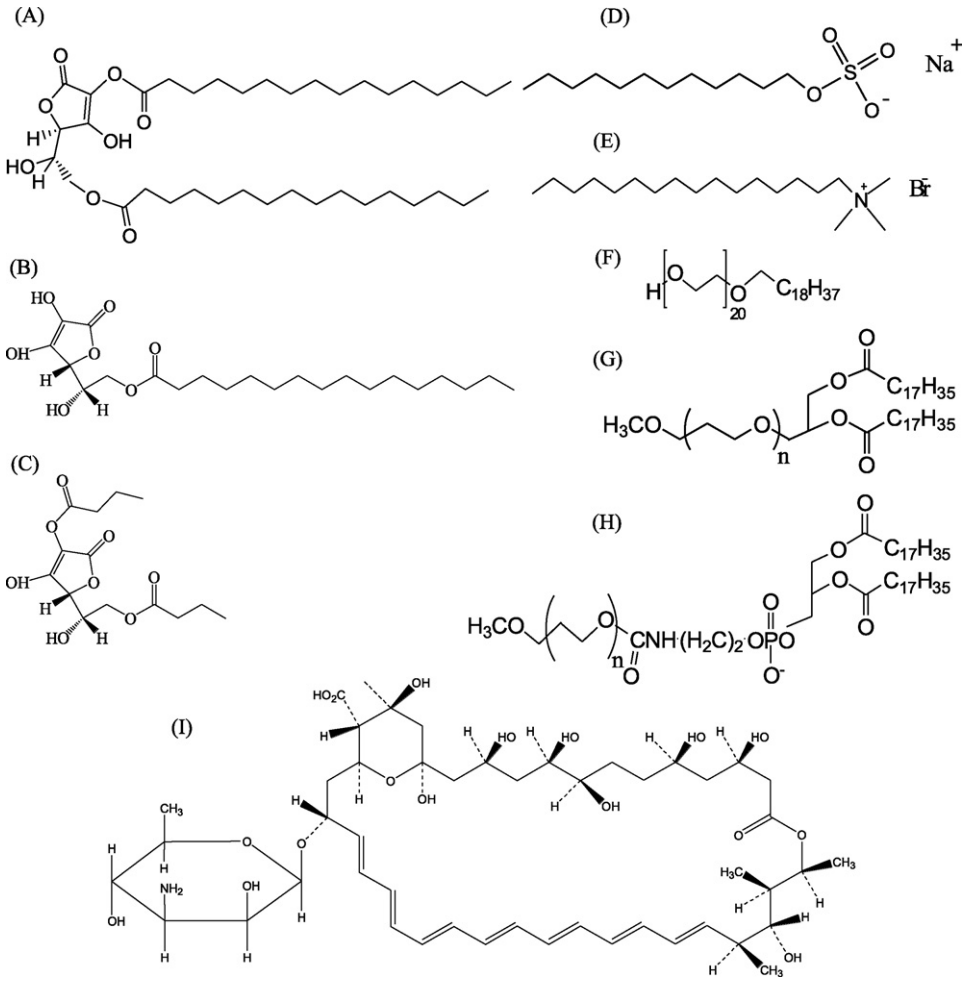

Fig. 1. Chemical structure of ascorbyl-2,6-dipalmitate (ASC-DP), surfactants, and amphotericin B (AmB). (A) ASC-DP, (B) ascorbyl-6-palmitate (ASC-P), (C) ascorbyl-2,6-dibutyrate (ASC-DB), (D) sodium dodecyl sulfate (SDS), (E) cetyltrimethyl ammonium bromide (CTAB), (F) polyoxyethylene stearyl ether (Brij®78), (G) distearoyl glycerol PEG 2000 (DSG-PEG), (H) distearoylphosphatidylethanolamine polyethylene glycol 2000 (DSPE-PEG), and (I) AmB.

2.10. Blood residence in vivo

Fungizone® and the AmB/ASC-DP/DSPE-PEG nanoparticle suspension were intravenously injected to the mice via the tail vain at a dose of 1.0 mg AmB/kg body weight. At desired time intervals, blood samples were collected from the anesthetized mice by cardiac puncture, and serum samples were separated by centrifugation. The serum sample (500 μL) was mixed with an extracting reagent (10-mM phosphate buffer, pH 7.4, 1 mL), an internal standard solution (4-nitro-1-naphthylamine, 10 μg/mL, 1.0 mL), and methanol (3.0 mL). Serum proteins were separated by centrifugation. The AmB in the serum was extracted from the supernatant using C18 BOND-ELUT® (Varian, CA, USA), eluted with 1.0 mL of acetonitrile-2.5 mM Na_2EDTA (60/40, v/v), and measured by means of high-pressure liquid chromatography. A Wakosil C18 column (4.6 mm × 150 mm, Wako Pure Chemicals, Japan) was used, and the mobile phase was acetonitrile—10 mM AcOH (pH 4.0) (11/17, v/v) with a flow rate of 0.7 mL/min. AmB and the internal standard had retention times of 6.0 and 9.0 min, respectively. The absorbance of the column effluent was measured at 385 nm. The area under the plasma concentration–time curve (AUC) value (0–4 h) of the plasma profiles was calculated using logarithmic and linear trapezoidal rules. P values were calculated using the *F*-test ($p = 0.023$) and *t*-test ($p = 0.036$), and values less than 0.05 were considered significant.

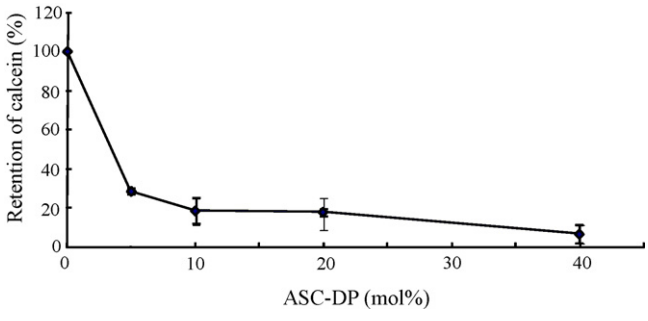

Fig. 2. Retention of calcein (%) in ASC-DP-incorporated DSPC liposomes. Each point represents the mean ± SD ($n = 3$).

3. Results and discussion

3.1. Physicochemical properties of ASC-DP

The chemical structure of the excipients used in this study is shown in Fig. 1. It has been reported that ASC-P forms micelles because of its intrinsic surface-active properties. ASC-P is miscible with phospholipids, forming a mixed lamellar structure (Gopinath et al., 2004). In contrast, ASC-DP is poorly soluble in water. At first, we attempted to encapsulate calcein by hydrating ASC-DP films. However, no vesicles were formed. Calcein was used as

a hydrophilic fluorescent probe encapsulated in the inner water phase of vesicles. The miscibility of ASC-DP with phospholipids was investigated to determine its vesicle-forming ability. Fig. 2 shows that in the presence of ASC-DP, the DSPC liposomes retain calcein. Calcein retention (%) in ASC-DP-containing DSPC liposomes dramatically decreased with the incorporation of 5–10 mol% ASC-DP. The release of calcein indicated that the DSPC bilayer structure was degraded after the incorporation of ASC-DP. These results indicate that the 2 acyl chains of ASC-DP cannot order into the lamellar structure.

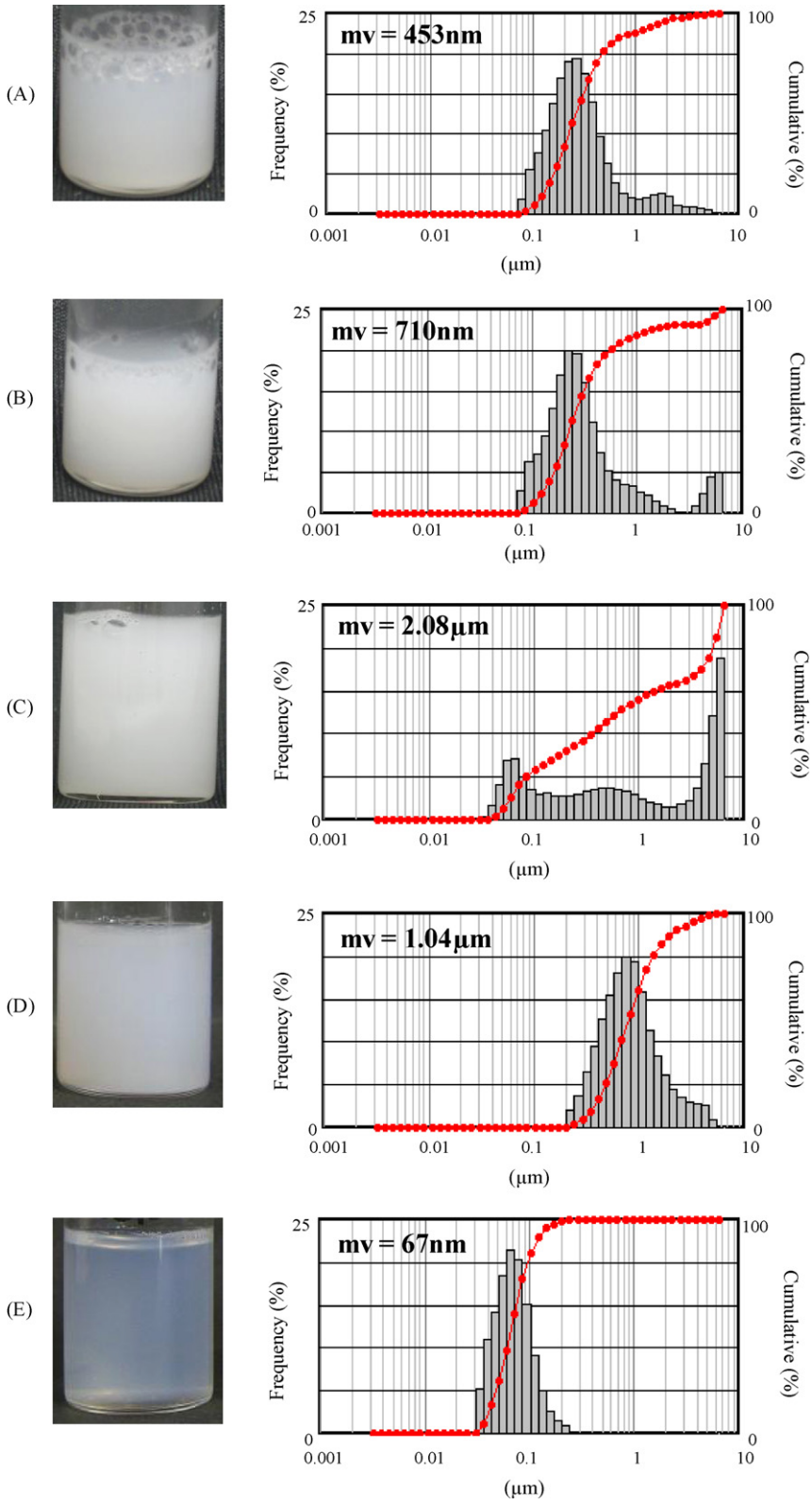

Fig. 3. Sample appearances and particle size distribution patterns of ASC-DP/surfactant (1:1 molar ratio) suspensions. The surfactants used were (A) SDS, (B) CTAB, (C) Brij®78, (D) DSG-PEG, and (E) DSPE-PEG.

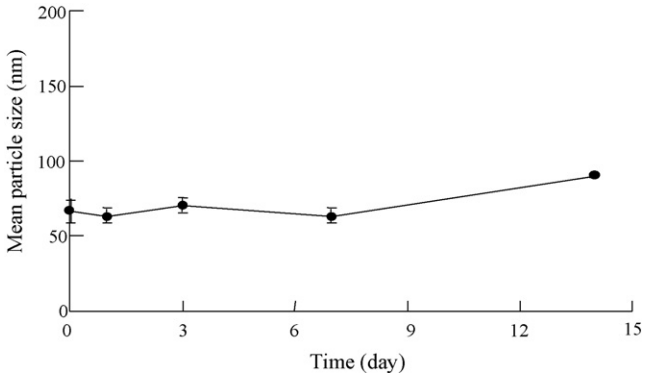

Fig. 4. Changes in the mean particle size of ASC-DP/DSPE-PEG nanoparticles after storage at 25 °C. Each point represents the mean ± SD (n = 3).

3.2. ASC-DP/DSPE-PEG nanoparticles

We attempted to combine ASC-DP and a surfactant in order to formulate a nano-sized drug carrier having ASC-DP as a component. Sample appearance and particle size distribution of the ASC-DP/surfactant (1:1 molar ratio) suspensions prepared by film hydration are shown in Fig. 3. The ASC-DP/SDS and ASC-DP/CTAB suspensions were white and turbid. The negative and positive charges of SDS and CTAB did not contribute to the solubilization of ASC-DP and subsequent stabilization of the formulation. Formation of nano-sized particles was observed with a non-ionic surfactant, Brij®78, although micron-sized particles also existed. Among the PEG-lipid derivatives, it was found that DSPE-PEG could form nano-sized particles with ASC-DP. The mean particle size of the ASC-DP/DSPE-PEG formulation was ca. 67 nm. The nanosuspensions were stable after storage.

As shown in Fig. 4, the mean particle size was almost constant after 7 days of storage, and did not exceed 100 nm after 2 weeks of storage. Its long-term stability may be attributed to the surface properties of the nanoparticles. The surface charge on the ASC-DP/DSPE-PEG nanoparticles was evaluated by zeta potential measurement and found to be −39.0 ± 4.3 mV (n = 3). The intrinsic negative charges of DSPE-PEG, presence of the PEG chain, and the structure of the spacer linking PEG and the phospholipid appeared to contribute to the stability of the nanoparticles that were formed. We assumed that ASC-DP solubilized and interacted with DSPE-PEG to form the nanoparticles.

The effect of the chemical structure of ascorbic-acid derivatives on nanoparticle formation with DSPE-PEG was also investigated. In the case of ASC-P, the mean particle size was 10 nm at first, indicating that ASC-P solubilized or formed mixed micelles with DSPE-PEG. ASC-DB, which has shorter acyl chains than ASC-DP and is poorly soluble in water, was solubilized by DSPE-PEG. However, precipitates of the complex were observed in both compositions after they had been storage for 24 or 72 h. These results indicate that ASC-P and ASC-DB cannot form stable nanosuspensions with DSPE-PEG. From the results of ^{13}C solid state NMR spectra, peak shift of C_2 carbon of ASC-DP was observed in ASC-DP/DSPE-PEG film (data not shown). Acyl chain length of ascorbic-acid derivatives appears to affect the hydrophobic interaction with DSPE-PEG with stearyl acyl chains. Thus, the chemical structure of the ascorbic-acid derivatives played an important role in stabilizing the nanoparticles formed with DSPE-PEG.

3.3. Drug/ASC-DP/DSPE-PEG nanoparticles

We tried to incorporate hydrophobic drugs into the ASC-DP/DSPE-PEG nanoparticles. The mean particle size of the drug (10 mol%)-containing DSPE-PEG micelles or ASC-DP/DSPE-PEG (1:1 molar ratio) nanoparticles is summarized in Table 1. DSPE-PEG micelles formed drug-containing nanoparticles, except for with nystatin and fluconazole (>1.0 μm). However, drug precipitates or large-sized drug particles were observed after the system was stored for 24 h. DSPE-PEG could reduce the size of the drug to the submicron order, although its stability in water was extremely low. In the case of the drug/ASC-DP/DSPE-PEG ternary system, the particle size was less than 200 nm with each drug. Furthermore, no variation in particle size was observed after storage for 24 h. Thus, combining ASC-DP with DSPE-PEG resulted in the formation of stable drug-containing nanoparticles.

Table 1
The mean particle size of the drug (10 mol%)-containing DSPE-PEG micelles or ASC-DP/DSPE-PEG (1:1 molar ratio) nanoparticles.

Drug	Mean particle size (nm)		
	DSPE-PEG micelle	ASC-DP/DSPE-PEG nanoparticle	
		After hydration	After storage for 24 h
Amphotericin B	129[a]	170	162
Nystatin	1360[a]	125	120
Fluconazole	1380[b]	79	76
Clarithromycin	282[b]	133	126
Acetohexamide	331[b]	189	159
Vitamin D_3	376[b]	90	89
Coenzyme Q_{10}	207[b]	102	96
Thioctic acid	312[b]	80	80

[a] Mean particle size after the storage for 24 h. Drug was solubilized at first but gradually agglomerated. Precipitates or particles larger than 1 μm were observed after the storage.
[b] Precipitates or particles larger than 1 μm were observed after hydration of the film.

Among the drugs shown in Table 1, AmB was selected as the model drug to be encapsulated in the ASC-DP/DSPE-PEG complex for further experiments. Since AmB interacts with DSPE-PEG (Moribe et al., 1998), it may be effectively incorporated by the ASC-DP/DSPE-PEG nanoparticles. The mean particle size and zeta potential of the ASC-DP/DSPE-PEG and AmB/ASC-DP/DSPE-PEG nanoparticles are shown in Table 2. Entrapment efficacy of AmB, which was evaluated by passing the sample solution through 0.8 μm filter, was more than 99% in each sample. Compared with the ASC-DP/DSPE-PEG nanoparticles, the mean particle size increased when AmB was incorporated. Particle size also increased with the amount of AmB incorporated. AmB-loaded nanoparticles were stable for at least 24 h. The zeta potential of the AmB-loaded nanoparticles remained negative, although it decreased slightly with increased incorporation of AmB. Surface charge of particle contributes to the electrostatic repulsion between particles dispersed in water. PEG aqueous layer formed on the particle surface

Table 2
Mean particle size and zeta potential of ASC-DP/DSPE-PEG and AmB/ASC-DP/DSPE-PEG nanoparticles.[a].

Sample	Mean particle size (nm)[b]		Zeta potential[c] (mV)
	After hydration	Storage for 24 h	
ASC-DP/DSPE-PEG	67 ± 7	63 ± 5	−39.0 ± 4.3
AmB (1 mol%)/ASC-DP/DSPE-PEG	122 ± 8	122 ± 8	−37.2 ± 1.4
AmB (5 mol%)/ASC-DP/DSPE-PEG	135 ± 2	157 ± 3	−32.6 ± 0.6
AmB (10 mol%)/ASC-DP/DSPE-PEG	170 ± 7	163 ± 5	−33.9 ± 0.4
AmB (20 mol%)/ASC-DP/DSPE-PEG	198 ± 5	185 ± 6	−30.7 ± 0.3

[a] Entrapment efficacy of AmB, which was evaluated by passing the sample solution through 0.8-mm filter, was more than 99% in each samples.
[b] Mean ± SD, n = 3.
[c] Mean ± SD, n = 5.

Table 3
The minimum lethal dose of the AmB/ASC-DP/DSPE-PEG, AmB/DSPE-PEG micelles, and Fungizone® ($n = 3–5$).

	AmB (10 mol%)/ASC-DP/DSPE-PEG	AmB (10 mol%)/DSPE-PEG	Fungizone®
Injected dose (mg AmB/kg body weight)	10.0	2.0	3.0

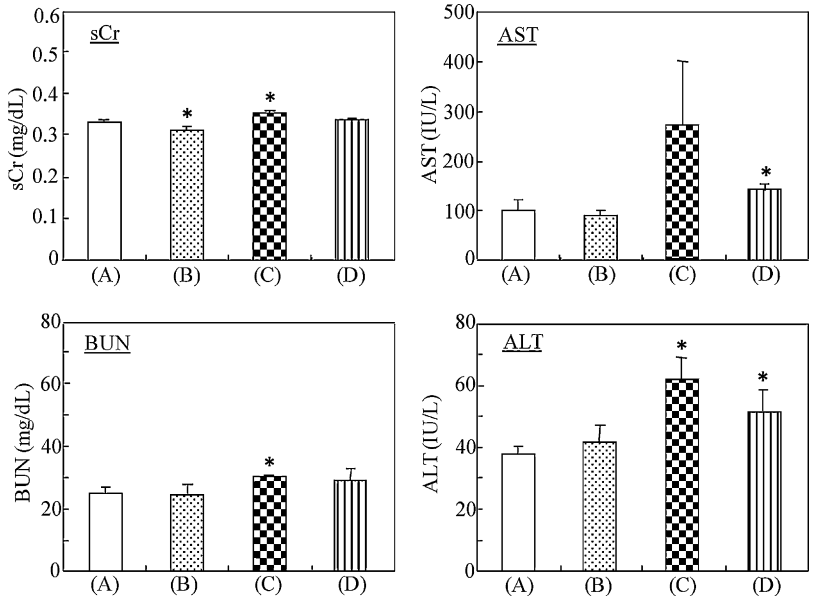

Fig. 5. Effect of the AmB formulation on sCr, BUN, AST, and ALT values at 48 h after injection. (A) Control, (B) AmB (10 mol%)/ASC-DP/DSPE-PEG, (C) AmB (10 mol%)/DSPE-PEG micelle, and (D) Fungizone®. Each bar represents the mean ± SD ($n = 3$). Samples were injected via the mouse tail vain at a dose of 1.0 mg AmB/kg body weight. *$p < 0.05$, significant differences between the control and the AmB/ASC-DP/DSPE-PEG micelles, AmB/DSPE-PEG micelles, and Fungizone®.

avoids the contact between particles. It was speculated that the surface charges and PEG coverage may contribute to the stable nanoparticle formation.

3.4. Toxicity tests in animal models

The main adverse reactions to AmB formulations were hepatic and renal disorders. Acute toxicity was evaluated in terms of MLD and hepatic and renal toxicities. Table 3 shows the MLD of the AmB/ASC-DP/DSPE-PEG and AmB/DSPE-PEG micelles and Fungizone® ($n = 3–5$). The MLD of the AmB (10 mol%)/ASC-DP/DSPE-PEG nanoparticles was 10 mg/kg, which was more than 3 times that of Fungizone® (3 mg/kg) and the AmB (10 mol%)/DSPE-PEG micelles (2 mg/kg). When an unstable micelle formulation is administered intravenously, it is degraded by dilution and the subsequent drug release, following which drug aggregation occurs. We speculated that degradation of the unstable AmB/DSPE-PEG micelles and aggregation of the released AmB appeared to be why

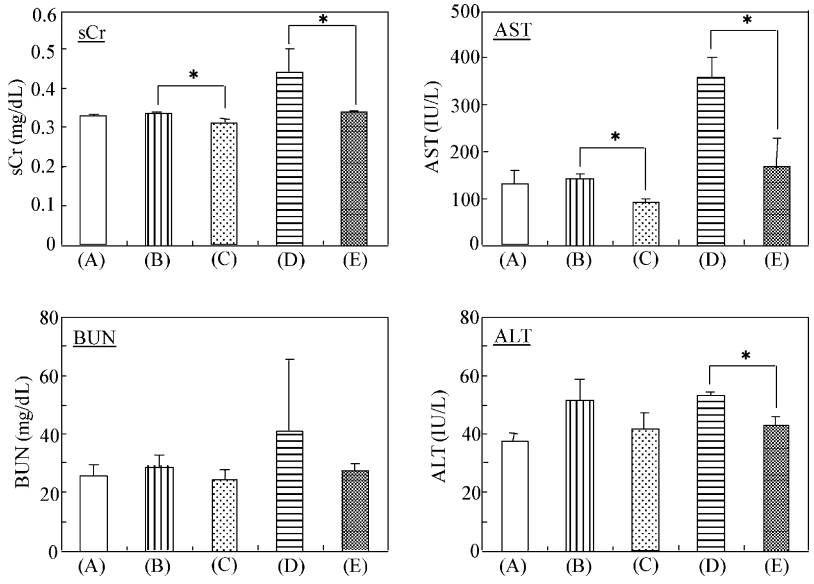

Fig. 6. Effect of dose of AmB injected on sCr, BUN, AST, and ALT values at 48 h after injection of each formulation. (A) Control, (B) Fungizone® (1.0 mg/kg), (C) AmB (10 mol%)/ASC-DP/DSPE-PEG (1.0 mg/kg), (D) Fungizone® (2.0 mg/kg), and (E) AmB (10 mol%)/ASC-DP/DSPE-PEG (2.0 mg/kg). Each bar represents the mean ± SD ($n = 3$). Samples were injected via the mouse tail vain. *$p < 0.05$, significant differences between AmB/ASC-DP/DSPE-PEG and Fungizone®.

Table 4
The pharmacokinetic parameters of plasma AmB after mice were intravenously administered the AmB/ASC-DP/DSPE-PEG nanoparticles or Fungizone® at the same dose of 1.0 mg/kg (n = 3–5).

	CL_{tot} (mL/g h)	$t_{1/2}$ (h)	C_0 (μg/mL)	V_d (mL/g)	$AUC_{0-4\,h}$ (μg h/mL)
AmB (10 mol%)-nanoparticle	0.078	1.18	7.55	0.132	21.7*
Fungizone®	0.147	0.811	5.83	0.172	11.4

* $p < 0.05$, significant differences between AmB/ASC-DP/DSPE-PEG and Fungizone®.

the AmB/DSPE-PEG micelles had the highest toxicity. Similar phenomena might occur with Fungizone®. ASC-DP, however, could stabilize the DSPE-PEG micelle formulation.

Effects of the AmB formulation on sCr, BUN, AST, and ALT levels were determined 2 days after injection. As shown in Fig. 5, when AmB was administered at a dose of 1.0 mg AmB/kg body weight, treatment with the AmB/ASC-DP/DSPE-PEG nanoparticles was associated with lower hepatic and renal toxicities than treatment with the AmB/DSPE-PEG micelles and Fungizone®. Compared with the control, a significant increase in toxicity was observed in terms of sCr and BUN levels after the AmB/DSPE-PEG micelle formulation was administered, in terms of AST levels after Fungizone® was administered, and in terms of ALT levels after the AmB/DSPE-PEG micelle formulation and Fungizone® were administered. Therefore, we conclude that the ASC-DP in the AmB formulation helped reduce hepatic and renal toxicities.

We also investigated the dose-related effect of the AmB/ASC-DP/DSPE-PEG nanoparticles on the hepatic and renal toxicities at 2 days after the injection. As shown Fig. 6, the sCr and AST levels after the AmB/ASC-DP/DSPE-PEG nanoparticles (C and E) in mice were significantly lower than that for Fungizone® administration (B and D), when the equivalent dose was administered. In general, the sCr level does not rise until at least half of the nephrons in kidney are damaged. Hepatic damage is also usually associated with elevated serum AST and ALT. A significant dose-related increase in the sCr and AST levels by Fungizone® means damage to a large number of nephrons and liver. While serum creatinine increases only with nephron damage, the BUN is affected by hydration, hepatic metabolism of protein, and reduced glomerular filtration rate. Although Fungizone® treatment (B and D) did not induce a statistically significant change in the BUN and ALT levels (except for ALT with 2.0 mg/kg), the result indicated a slight increase in indicators of hepatic and renal toxicities after Fungizone® administration. However, even the high dose of AmB/ASC-DP/DSPE-PEG nanoparticles (E) appeared to reduce the levels of BUN and ALT. Therefore, it was suggested that the AmB/ASC-DP/DSPE-PEG nanoparticles is possible to use safely, without causing the biochemical abnormalities of the liver and kidney. To precisely evaluate the renal toxicity of AmB/ASC-DP/DSPE-PEG nanoparticles, further studies such as histopathological examination of kidney sections may be required.

3.5. Blood residence of AmB

Blood residence of AmB in nanoparticles and in Fungizone® was compared. Fig. 7 shows the plasma concentration–time profile of AmB after mice were intravenously administered the AmB/ASC-DP/DSPE-PEG nanoparticles or Fungizone® at the same dose of 1.0 mg/kg. The pharmacokinetic parameters were calculated and are presented in Table 4. As compared with the rapid disappearance of AmB after Fungizone® was administered, AmB administered in the form of AmB (10 mol%)/ASC-DP/DSPE-PEG nanoparticles was eliminated slowly from the plasma, with a half-life of 1.2 h. The plasma level of AmB with the AmB (10 mol%)/ASC-DP/DSPE-PEG nanoparticles was always higher than that with Fungizone® at the corresponding time. A significant increase in AUC was observed with the AmB/ASC-DP/DSPE-PEG nanoparticles as compared with

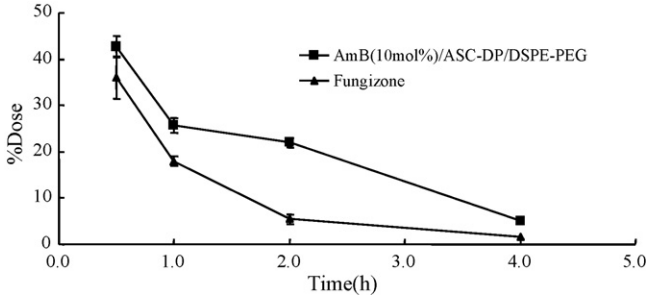

Fig. 7. Plasma concentration of AmB after mice were intravenously administered AmB/ASC-DP/DSPE-PEG nanoparticles or Fungizone® at a dose of 1.0 mg/kg. Each point represents the mean ± SD (n = 3–5).

Fungizone® ($p < 0.05$). These results suggest that the ASC-DP/DSPE-PEG nanoparticles play a role in delaying the disappearance of AmB from tissues such as the liver and kidney. The presence of PEG on the surface of nanoparticles may contribute to the increased blood residence of the drug. On the basis of these results, the ASC-DP/DSPE-PEG nanoparticles appear to be a candidate AmB carrier.

Composition of the ternary components as well as intermolecular interactions among the components influenced the structure and stability of the nanoparticles. To increase the blood residence of drug/ASC-DP/DSPE-PEG nanoparticles, composition and structure need to be optimized. In terms of drug selection, those that interact with ASC-DP or DSPE-PEG should be chosen since these drugs are incorporated into the nanoparticles after interaction. Physicochemical characterization of drug/ASC-DP/DSPE-PEG nanoparticles is underway and will be discussed in a subsequent paper.

4. Conclusion

Combining ASC-DP and DSPE-PEG enabled stable nanoparticle formation. AmB and other hydrophobic drugs were successfully loaded onto the ASC-DP/DSPE-PEG nanoparticle system. Compared with Fungizone®, a solubilized AmB formulation with sodium deoxycholate, the toxicity and blood residence of the ASC-DP/DSPE-PEG nanoparticles was significantly better when administered intravenously to mice. ASC-DP incorporation is believed to contribute not only to stabilization of the nanoparticles but also to the antioxidation property of the formulation. Since ASC-DP has been used in cosmetics, drug-nanoparticle formulations with ASC-DP can be administered by alternative routes, such as transdermal or mucoadhesive routes. In conclusion, ASC-DP/DSPE-PEG nanoparticles appear to be a promising delivery system for hydrophobic drugs.

Acknowledgements

This research was supported by a Grant-in-Aid from the Ministry of Education, Culture, Sports, Science and Technology (Monbukagakusho) of Japan (21590038), the Japan Health Sciences Foundation, Cosmetology Research Foundation, Japan, and in part by the Mochida Memorial Foundation, Japan.

References

Bilia, A.R., Bergonzi, M.C., Vincieri, F.F., Nostro, P.L., Morris, G.A., 2002. A diffusion-ordered NMR spectroscopy study of the solubilization of artemisinin by octanoyl-6-*O*-ascorbic acid micelles. J. Pharm. Sci. 91, 2265–2270.

Fočo, A., Gašperlin, M., Kristl, J., 2005. Investigation of liposomes as carriers of sodium ascorbyl phosphate for cutaneous photoprotection. Int. J. Pharm. 291, 21–29.

Gopinath, D., Ravi, D., Rao, B.R., Apte, S.S., Renuka, D., Rambhau, D., 2004. Ascorbyl palmitate vesicles (Aspasomes): formation, characterization and applications. Int. J. Pharm. 271, 95–113.

Inoue, Y., Yoshimura, S., Tozuka, Y., Moribe, K., Kumamoto, T., Ishikawa, T., Yamamoto, K., 2007. Application of ascorbic acid 2-glucoside as a solubilizing agent for clarithromycin: solubilization and nanoparticle formation. Int. J. Pharm. 331, 38–45.

Lien, M.H., Huang, B.C., Hsu, M.C., 1993. Determination of ascorbyl dipalmitate in cosmetic whitening powders by liquid chromatography. J. Chromatogr. 645, 362–365.

Llabot, J.M., Palma, S.D., Manzo, R.H., Allemandi, D.A., 2007. Design of novel antifungal mucoadhesive films. Part I: Pre-formulation studies. Int. J. Pharm. 330, 54–60.

LoNostro, P., Capuzzi, G., Pinelli, P., Mulinacci, N., Romani, A., Vincieri, F.F., 2000. Self-assembling and antioxidant activity of some vitamin C derivatives. Colloid. Surf. Physicochem. Eng. Aspect. 167, 83–93.

Matsukawa, H., Yagi, T., Matsuda, H., Kawahara, H., Yamamoto, I., Matsuoka, J., Tanaka, N., 2000. Ascorbic acid 2-glucoside prevents sinusoidal endothelial cell apoptosis in supercooled preserved grafts in rat liver transplantation. Transplant. Proc. 32, 313–317.

Moribe, K., Tanaka, E., Maruyama, K., Iwatsuru, M., 1998. Enhanced encapsulation of amphotericin B into liposomes by complex formation with polyethylene glycol derivatives. Pharm. Res. 15, 1737–1742.

Nishiyama, N., Kataoka, K., 2006. Current state, achievements, and future prospects of polymeric micelles as nanocarriers for drug and gene delivery. Pharmacol. Ther. 112, 630–648.

Ratnam, D.V., Ankola, D.D., Bhardwaj, V., Sahana, D.K., Ravi Kumar, M.N.V., 2006. Role of antioxidants in prophylaxis and therapy: a pharmaceutical perspective. J. Control. Release 113, 189–207.

Sawant, R.M., Hurley, J.P., Salmaso, S., Kale, A., Tolcheva, E., Levchenko, T.S., Torchilin, V.P., 2006. "SMART" drug delivery systems: double-targeted pH-responsive pharmaceutical nanocarriers. Bioconjug. Chem. 17, 943–949.

Špiclin, P., Gašperlin, M., Kmetec, V., 2001. Stability of ascorbyl palmitate in topical microemulsions. Int. J. Pharm. 222, 271–279.

Takebayashi, J., Tai, A., Gohda, E., Yamamoto, I., 2006. Characterization of the radical-scavenging reaction of 2-*O*-substituted ascorbic acid derivatives, AA-2G, AA-2P, and AA-2S: a kinetic and stoichiometric study. Biol. Pharm. Bull. 29, 766–771.

Tanaka, H., Yamamoto, R., 1996. Pharmaceutical studies on ascorbic acid derivatives. Yakugakuzasshi 86, 376–383.

Teeranachaideekul, V., Junyaprasert, V.B., Souto, E.B., Müller, R.H., 2008. Development of ascorbyl palmitate nanocrystals applying the nanosuspension technology. Int. J. Pharm. 354, 227–234.

Yamada, Y., Harashima, H., 2008. Mitochondrial drug delivery systems for macromolecule and their therapeutic application to mitochondrial diseases. Adv. Drug Deliv. Rev. 60, 439–462.

Yamamoto, H., Kuno, Y., Sugimoto, S., Takeuchi, H., Kawashima, Y., 2005. Surface-modified PLGA nanosphere with chitosan improved pulmonary delivery of calcitonin by mucoadhesion and opening of the intercellular tight junctions. J. Control. Release 102, 373–381.

Yamamoto, I., Muto, N., Nagata, E., Nakamura, T., Suzuki, Y., 1990. Formation of a stable l-ascorbic acid α-glucoside by mammalian α-glucosidase-catalyzed transglucosylation. Biochim. Biophys. Acta 1035, 44–50.